Synthesis and Optical Properties of Copolymers Containing Side Chain Oxadiazole Blocks and a Rigid Central Moiety

Nikos P. Tzanetos and Joannis K. Kallitsis*

Department of Chemistry, University of Patras, GR-265 00 Patras, Greece, and Institute of Chemical Engineering and High-Temperature Chemical Processes (ICE/HT), GR-265 00 Patras, Greece

Received March 1, 2004. Revised Manuscript Received April 22, 2004

Rod−coil block copolymers containing di(styryl)-anthracene units as the rod block and oxadiazole homopolymers as the flexible blocks are reported. These copolymers were synthesized by atom transfer radical polymerization (ATRP) of the desired oxadiazole monomers using a properly modified conjugated segment as initiator. The resulting copolymers were obtained in high yields and with very narrow polydispersities down to 1.17 in some cases and were primarily characterized by using size exclusion chromatography (GPC) and spectroscopic (^{1}H NMR) and thermal (DSC) techniques. Additionally, their optical properties were investigated in detail and were found to emit in the green spectral region in the solid state resulting from an efficient energy transfer from the oxadiazole to the anthracene type chromophores.

Introduction

Copolymers consisting of hole-transporting and electron-transporting segments are currently of interest because a balanced mobility of the different charge carriers is needed in optoelectronic devices.[1,2] Such copolymers having various donor−acceptor architectures can extend to systems with efficient photoinduced charge transfer and separation for photovoltaic devices and to bipolar charge transport materials for light-emitting diodes,[3] lasers,[4] and other applications.[5] Most conjugated polymers are hole-transporting materials because of their chemical nature, that is, extented π-electron delocalization. To obtain highly efficient PLED devices, a balance in the injection of holes and electrons into the polymer emissive layer is necessary. Therefore, attention has been given to the development of polymers with improved electron transport capability.[6] Moreover, the discovery of photoinduced electron transfer from conjugated polymers to fullerene solid composites[7] as an electron-accepting material stimulated an intensive research effort toward the development of soluble fullerene derivatives[2,8] as well as other alternative structures.[1a,9−11]

Oxadiazoles are one of the first and most extensively investigated class of electron-accepting materials.[3a,3c,3d] The oxadiazole unit is an electron-deficient heterocyclic ring, thus making 1,3,4-oxadiazole derivatives extremely poor hole acceptors. 1,3,4-Oxadiazole derivatives, such as 2-(4-biphenylyl)-5-(4-*tert*-butylphenyl)-1,3,4-oxadiazole (PBD), have long been some of the most favorable compounds in organic light-emitting diodes (OLEDs).[12−14] However, in most cases the OLEDs efficiency was limited due to the oxadiazoles incompat-

* Corresponding author.

(1) (a) Boiteau, L.; Moroni, M.; Hilberer, A.; Werts, M.; de Boer, B.; Hadziioannou, G. *Macromolecules* **2002**, *35*, 1543. (b) Jiang, X. Z.; Register, R. A.; Killeen, K. A.; Thomson, M. E.; Pschenitzka, F.; Sturm, J. C. *Chem. Mater.* **2000**, *12*, 2542. (c) Hwang, S. W.; Chen, Y. *Macromolecules* **2002**, *35*, 5438. (d) Zhan, X.; Liu, Y.; Wu, X.; Wang, S.; Zhu, D. *Macromolecules* **2002**, *35*, 2529.

(2) (a) Stalmach, U.; de Boer, B.; Videlot, C.; van Hutten, P. F.; Hadziioannou, G. *J. Am. Chem. Soc.* **2000**, *122*, 5464. (b) de Boer, B.; Stalmach, U.; van Hutten, P. F.; Melzer, C.; Krasnikov, V. V.; Hadziioannou, G. *Polymer* **2001**, *42*, 9097.

(3) (a) Kraft, A.; Grimsdale, A. C.; Holmes, A. B. *Angew. Chem., Int. Ed.* **1998**, *37*, 402. (b) Zhang, X.; Jenekhe, S. A. *Macromolecules* **2000**, *33*, 2069. (c) Kim, D. Y.; Cho, H. N.; Kim, C. Y. *Prog. Polym. Sci.* **2000**, 25, 1089. (d) Akcelrud, L. *Prog. Polym. Sci.* **2003**, *28*, 875.

(4) McGehee, M. D.; Heeger, A. J. *Adv. Mater.* **2000**, *12*, 1655.

(5) Heeger, A. J. *J. Phys. Chem. B.* **2001**, *105*, 8475.

(6) (a) Ding, J.; Day, M.; Robertson, G.; Roovers, J. *Macromolecules* **2002**, *35*, 3474. (b) Pei, Q.; Yang, Y. *Chem. Mater.* **1995**, *7*, 1568. (c) Hsiao, S.-H.; Yu, C.-H. *J. Polym. Sci., Part A: Polym. Chem.* **1998**, *36*, 1847. (d) Peng, Z.; Bao, Z.; Galvin, M. E. *Chem. Mater.* **1998**, *10*, 2086. (e) Peng, Z.; Bao, Z.; Galvin, M. E. *Adv. Mater.* **1998**, *10*, 680. (f) Peng, Z.; Zhang, J. *Chem. Mater.* **1999**, *11*, 1138. (g) Yu, W.-L.; Meng, H.; Pei, J.; Huang, W.; Li, Y.; Heeger, A. J. *Macromolecules* **1998**, *31*, 4838.

(7) (a) Sariciftci, N. S.; Smilowitz, L.; Heeger, A. J.; Wudl, F. *Science* **1992**, *258*, 1474. (b) Brabec, C. J.; Sariciftci, N. S.; Hummelen, J. C. *Adv. Funct. Mater.* **2001**, *11*, 15. (c) Brabec, C. J.; Sariciftci, N. S. In *Semiconducting Polymers*; Hadziioannou, G., van Hutten, P. F., Eds.; Wiley−VCH: Weinheim, 1999; Chapter 15, pp 515−560. (d) Sariciftci, N. S.; Heeger A. J. In *Handbook of Organic Conductive Molecules and Polymers*; Nalwa, H. S., Ed.; John Wiley & Sons: New York, 1997; Vol. 1.

(8) (a) Hummelen, J. C.; Knight, B. W.; LePec, F.; Wudl, F. *J. Org. Chem.* **1995**, *60*, 532. (b) Cravino, A.; Sariciftci, N. S. *J. Mater. Chem.* **2002**, *12*, 1931. (c) Eckert, J.-F.; Nicoud, J.-F.; Nierengarten, J.-F.; Liu, S.-G.; Echegoyen, L.; Barigelletti, F.; Armaroli, N.; Ouali, L.; Krasnikov, V.; Hadziioannou, G. *J. Am. Chem. Soc.* **2000**, *122*, 7467. (d) Ramos, A. M.; Rispens, M. T.; van Duren, J. K. J.; Hummelen, J. C.; Janssen, R. A. J. *J. Am. Chem. Soc.* **2001**, *123*, 6714. (e) Zhang, F.; Svensson, M.; Andersson, M. R.; Maggini, M.; Bucella, S.; Menna, E.; Inganäs, O. *Adv. Mater.* **2001**, *13*, 1871.

(9) Jonforsen, M.; Johansson, T.; Inganäs, O.; Andersson, M. R. *Macromolecules* **2002**, *35*, 1638.

(10) Alam, M. M.; Jenekhe, S. A. *J. Phys. Chem. B.* **2001**, *105*, 2479.

(11) Jenekhe, S. A.; Lu, L.; Alam, M. M. *Macromolecules* **2001**, *34*, 7315.

(12) Berggren, M.; Gustafsson, G.; Inganäs, O.; Andersson, M. R.; Hjertberg, T.; Wennerström, O. *J. Appl. Phys.* **1994**, *76*, 7530.

(13) Brown, A. R.; Bradley, D. D. C.; Burn, P. L.; Burroughes, J. H.; Friend, R. H.; Greenham, N. C.; Holmes, A. B.; Kraft, A. *Appl. Phys. Lett.* **1992**, *61*, 2793.

10.1021/cm049670k CCC: $27.50
Published on Web 05/27/2004

ibility with the other polymeric components that may lead to phase separation or crystallization phenomena especially at higher temperatures. Crystallization can be suppressed by covalently attaching the hole and electron transport moieties to the same copolymer.[1b,6d,6e,15]

As is well-known, the copolymer architecture plays a crucial role in the phase separation and consequently to the adopted morphology, but also to their miscibility behavior with other homopolymers. Since most of the luminescent polymers consist of a rigid polymeric backbone, a favorable architecture of interest is that of the rod−coil block copolymers.[2,16−18] These copolymers combine the advantages of polymers, such as easy processing and the absence of crystallization in the devices, with the advantages of the low molecular weight compounds, such as solubility, high purity, and a well-defined conjugation length. A proper combination of the structure of the rigid, conjugated segment and the coil part resulted in unique morphologies.[2a] Furthermore, block copolymers consisting of a block with donor functionality linked to a block with acceptor properties combined with the ability to self-organize into regular and ordered nanophases are ideal candidates for photovoltaic cells.[2] Incorporation of the anthracene unit into a polymeric backbone has been attempted to decrease the electronic gap of the polymer.[19,20] This is due to the fact that the incorporation of the anthracene unit into the polymer main chain should minimize the energy difference between the aromatic and quinoid resonance when compared to that of the 1,4-phenylene unit.[21,22]

In this work a rigid, bifunctional, and luminescent di(styryl)-anthracene-based initiator for the atom transfer radical polymerization (ATRP)[23] of various vinyl monomers was synthesized in satisfactory yields. This initiator was used for the preparation of coil−rod−coil copolymers that combine the anthracene derivative as the rigid block with moieties bearing oxadiazole units as the coil blocks through ATRP. Two different oxadiazole monomers, namely, 2-[4-(4-vinylbenzyloxy)-phenyl]-5-phenyl-1,3,4-oxadiazole[1b,24] (**I**) and 1-(4-vinylbenzyloxy)-3,5-bis[5-(phenyl)-2-oxadiazolyl]benzene (**II**),

Scheme 1. (i) BPO, THF or AIBN, DMF

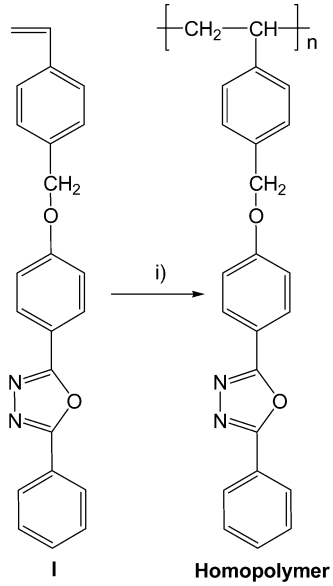

were used. All monomers and following copolymers synthesized have been fully characterized with ^{1}H NMR, GPC, and DSC techniques. The optical properties of these copolymers have been investigated in detail employing UV−visible and fluorescence techniques and were found to emit in the green spectral region in the solid state.

Experimental Section

Materials. Compounds **a**,[20] **b**,[25] and **c**,[1b,26] the monomer **I**,[1b,24] and the oxadiazole homopolymers[1b,24] (Scheme 1) were synthesized according to literature procedures. Diphenyl ether (Merck) was stored over molecular sieves (4 Å) and purged with argon for 30 min before the polymerization was started. CuBr (Aldrich), 2,2′-bipyridine (bipy, Aldrich), *N*,*N*,*N*′,*N*′,*N*″-pentamethyldiethylene triamine (PMDETA, Aldrich), and all the other reagents and solvents were used as received. All the polymerization reactions were carried out under an argon atmosphere.

Instrumentation. The structures of the synthesized copolymers were clarified by high-resolution ^{1}H NMR spectroscopy with a Bruker Avance DPX 400 MHz spectrometer. Molecular weights (M_n and M_w) were determined by gel permeation chromatography (Ultrastyragel columns with 500 and 10^4 Å pore size; $CHCl_3$ (analytical grade) was filtered through a 0.5-μm Millipore filter and samples were passed through a 0.2-μm Millipore filter; flow 1 mL min^{-1}; room temperature) using polystyrene standards for calibration. The UV spectra were recorded on a Hewlett-Packard 8452 A Diode Array UV−Visible spectrophotometer. Fluorescence was measured on an SLM Aminco SPF-500 spectrofluorometer. Differential scanning calorimetry (DSC) thermograms were obtained using a TA Instrument DSC Q100 Series. The heating rate was 20 °C min^{-1} for both first and second scans, in a temperature region from −50 to 300 °C.

3,5-Bis[5-(phenyl)-2-oxadiazolyl]phenol. 5-Acetoxyisophthaloyl chloride, 1.75 g (6.69 mmol), and 1.96 g (13.38 mmol) of phenyl tetrazole were dissolved in 40 mL of dry pyridine.

(14) (a) Adachi, C.; Tsutsui, T.; Saito, S. *Appl. Phys. Lett*. **1989**, 55, 1489. (b) Adachi, C.; Tsutsui, T.; Saito, S. *Appl. Phys. Lett.* **1990**, *56*, 799.

(15) Kido, J.; Harada, G.; Nagai, K. *Chem. Lett*. **1996**, 161.

(16) (a) Tsolakis, P. K.; Kallitsis, J. K. *Chem. Eur. J*. **2003**, *9*, 936. (b) Tsolakis, P. K.; Godt, A.; Kallitsis, J. K. *Macromolecules* **2002**, *35*, 5758.

(17) (a) Tew, G. N.; Pralle, M. U.; Stupp, S. I. *J. Am. Chem. Soc.* **1999**, *121*, 9852. (b) Gunther, J.; Stupp, S. I. *Langmuir* **2001**, *17*, 6530. (c) Stupp, S. I.; Lebonheur, V.; Walker, K.; Li, L.; Huggins, K. E.; Keser, M.; Amstutz, A. *Science* **1997**, *276*, 384. (d) Pralle, M. U.; Whitaker, C. M.; Braun, P. V.; Stupp, S. I. *Macromolecules* **2000**, *33*, 3550. (e) Zubarev, E. R.; Pralle, M. U.; Li, L.; Stupp, S. I. *Science* **1999**, *283*, 523. (f) Hempenious, M. A., Langevelt-Voss, B. M. W.; van Haare, J. A. E. H.; Janssen, R. A. J.; Sheiko, S. S.; Spatz, J. P.; Möller, M.; Meijer, E. W. *J. Am. Chem. Soc.* **1998**, *120*, 2798.

(18) (a) Jenekhe, S. A.; Chen, X. L. *Science* **1998**, *279*, 1903. (b) Jenekhe, S. A.; Chen, X. L. *Science* **1999**, *283*, 372.

(19) Paul, S.; Stein, S.; Knoll, W.; Müllen, K. *Acta Polym*. **1994**, *45*, 235.

(20) Konstandakopoulou, F. D.; Kallitsis, J. *J. Polym. Sci., Part A: Polym. Chem*. **1999**, *37*, 3826.

(21) Weitzel, H.-P.; Bohnen, A.; Müllen, K. *Makromol. Chem*. **1990**, *191*, 2815.

(22) Ohlemacher, A.; Schenk, R.; Weitzel, H.-P.; Tyutyulkov, N.; Tasseva, M.; Müllen, K. *Makromol. Chem*. **1992**, *193*, 81.

(23) (a) Matyjaszewski, K. *Chem. Eur. J*. **1999**, *5*, 3095. (b) Matyjaszewski, K.; Xia, J. *Chem. Rev*. **2001**, *101*, 2921. (c) Kamigaito, M.; Ando, T.; Sawamoto, M. *Chem. Rev*. **2001**, *101*, 3689.

(24) (a) Jiang, X. Z.; Register, R. A.; Killeen, K. A.; Thomson, M. E.; Pschenitzka, F.; Hebner, T. R.; Sturm, J. C. *J. Appl. Phys*. **2002**, *91*, 6717. (b) Jiang, X. Z.; Jen, A. K.-Y.; Phelan, G. D.; Huang, D.; Londergan, T. M.; Dalton, L. R.; Register, R. A. *Thin Solid Films* **2002**, *416*, 212. (c) Jiang, X. Z.; Philan, G.; Carlson, B.; Liu, S.; Dalton, L.; Jen, A. K.-Y. *Macromol. Symp*. **2002**, *186*, 171.

(25) Greczmiel, M.; Strohriegl, P.; Meier, M.; Brütting, W. *Macromolecules* **1997**, *30*, 6042.

(26) Detert, H.; Schollmeier, D. *Synthesis* **1999**, No. *6*, 999.

After refluxing for 2 h under an argon atmosphere, the solution was cooled and poured into a mixture of 225 mL of distilled water and 45 mL of concentrated HCl. The precipitate was filtered off, washed with distilled water, and dried in a vacuum at 60 °C. Yield: 2.55 g (90%). 1.50 g (3.54 mmol) of the obtained product was dissolved in 80 mL of tetrahydrofuran and mixed with 0.71 g (17.70 mmol) of NaOH dissolved in 1.80 mL of water. After refluxing for 24 h, the reaction mixture was cooled and acidified with concentrated HC1. The solvent was evaporated and 80 mL of water was added to the crude product. After the mixture was stirred for 3 h, the white precipitate was filtered off, washed with water, and dried in a vacuum at 50 °C. Yield: 1.30 g (96%). ^{1}H NMR (DMSO-d_6): 7.63 (C_{Ar}**H**, d, 6H), 7.71 (C_{Ar}**H**, s, 2H), 8.14 (C_{Ar}**H**, d, 4H), 8.19 (C_{Ar}**H**, s, 1H), 10.7 ppm (O**H**, s, 1H).

1-(4-Vinylbenzyloxy)-3,5-bis[5-(phenyl)-2-oxadiazolyl]-benzene (II). A mixture of 3,5-bis[5-(phenyl)-2-oxadiazolyl]-phenol, 0.79 g (2.07 mmol), 4-vinylbenzyl chloride, 0.47 g (3.02 mmol), K_2CO_3, 0.57 g (4.14 mmol), and 18-crown-6, 0.11 g (0.41 mmol) in dry acetone (55 mL) was refluxed for 24 h under an argon atmosphere. After the mixture was cooled to room temperature, the resulting precipitate was filtered off, washed with water (3 × 30 mL), and dried in a vacuum at 60 °C. Excess 4-vinylbenzyl chloride was removed by triturating the product in hexane (20 mL). The product was then washed with additional hexane (3 × 5 mL) and dried under vacuum. Yield: 0.85 g (83%). ^{1}H NMR (DMSO-d_6): 5.25 (C**H**$_2$, d, 1H), 5.37 (OC**H**$_2$, s, 2H), 5.8 (C**H**$_2$, d, 1H), 6.74 (C**H**, q, 1H), 7.50 (C_{Ar}**H**, s, 4H), 7.64 (C_{Ar}**H**, m, 6H), 7.95 (C_{Ar}**H**, s, 2H), 8.16 (C_{Ar}**H**, d, 4H), 8.37 ppm (C_{Ar}**H**, s, 1H).

Preparation of the Initiator III. Triethylamine, 0.20 mL (1.47 mmol), and 2-chloropropionyl chloride (CPC), 0.29 mL (2.94 mmol), were added in three equal portions every 10 h to a cooled (ice bath) solution of 9,10-bis[p-hydroxystyryl] anthracene, 0.30 g (0.74 mmol), in 50 mL of tetrahydrofuran. The system was refluxed for 72 h after the last addition. The red solution was concentrated by evaporation of most of the solvent. Methanol (20 mL) was added to the residue and the yellow-green precipitate was isolated, washed with methanol, and dried under vacuum. Yield: 0.33 g (77%). ^{1}H NMR ($CDC1_3$): 1.88 (C**H**$_3$, d, 6H), 4.68 (C**H**, q, 2H), 6.93 (C**H**,d, 2H), 7.24 (C_{Ar}**H**, t, 4H), 7.49 (C_{Ar}**H**, q, 4H), 7.72 (C_{Ar}**H**, d, 4H), 7.91 (C**H**, d, 2H), 8.38 ppm (C_{Ar}**H**, q, 4H).

ATRP of Monomers Using the Rigid Initiator III. A round-bottom flask equipped with a rubber septum, a magnetic stirrer, and a gas inlet/outlet was flamed under vacuum. The initiator, 28.56 mg (0.048 mmol), was added to the flask containing CuBr, 13.77 mg (0.096 mmol), and PMDETA, 20 μL (0.096 mmol), or 2,2′-bipyridine, 30 mg (0.192 mmol). The system was degassed three times and flushed with argon. The solvent (2 mL) and different amounts of the desired monomers **I** or **II** as shown in Schemes 1 and 2 were added to the flask and the mixture was immediately degassed three times and flushed again with argon. The reaction mixture was then immersed in an oil bath and heated at 110 °C for 18 h. After the reaction mixture was cooled to room temperature, $CHCl_3$ (3−4 mL) was added to dissolve the polymer. The suspension was filtered for removal of most of the catalyst. The copolymers were precipitated in a large excess of methanol (20-fold excess by volume). The obtained copolymers were purified by reprecipitation from $CHCl_3$ into ethyl acetate or toluene and dried under vacuum at room temperature.

Results and Discussion

Monomer and Polymer Synthesis. Recent developments on controlled radical polymerization techniques enable the facile synthesis of various copolymer architectures. Among the different systems studied so far in the literature, ATRP combines easy experimental conditions with tolerance to different functional groups.[23] Moreover, ATRP is one of the most popular controlled radical polymerization methods to synthesize block copolymers and other complex macromolecular architectures of narrow dispersities and structural motives. The use of this technique for the synthesis of rod−coil copolymers has also been reported.[16] Schemes 1, 2, and 3 show the chemical structures of the monomers and copolymers synthesized in this study. Two kinds of copolymers containing a di(styryl)-anthracene unit as the rigid block and bearing one or two pendant oxadiazole units as the coil blocks were prepared by using ATRP. More specifically, the initiator **III** (Scheme 3) was synthesized and used for the polymerization of the oxadiazole monomer **I** and the monomer **II**, which contains two oxadiazole units, by ATRP, which resulted in triblock copolymers of the structures **1** and **2**. The unreacted initiator and monomers were effectively removed using disolution of the reaction mixture and precipitation in a good solvent for the initiator and monomers (toluene or ethyl acetate for the initiator, oxadiazole, and anthracene monomers). All of the copolymers exhibited good solubilities in a wide range of organic solvents, including $CHCl_3$, THF, and DMF. The high solubilities of the copolymers might be primarily due to the oxadiazole-based side groups of the flexible part of the copolymer as well as their relatively low molecular weights. Oxadiazole homopolymers[1b,24] with different molecular weights were also synthesized through free radical polymerization (Scheme 1). The structure of the initiator **III** was confirmed by ^{1}H NMR spectroscopy. The incorporation of the initiator into the polymeric chain and the initiation efficiency were also confirmed by ^{1}H NMR spectroscopy and gel permeation

Scheme 2. (i) NaN_3, NH_4Cl, DMF. (ii) 10 N NaOH, THF, HCl 37%. (iii) 4-Vinylbenzyl Chloride, K_2CO_3, 18-Crown-6, Acetone.

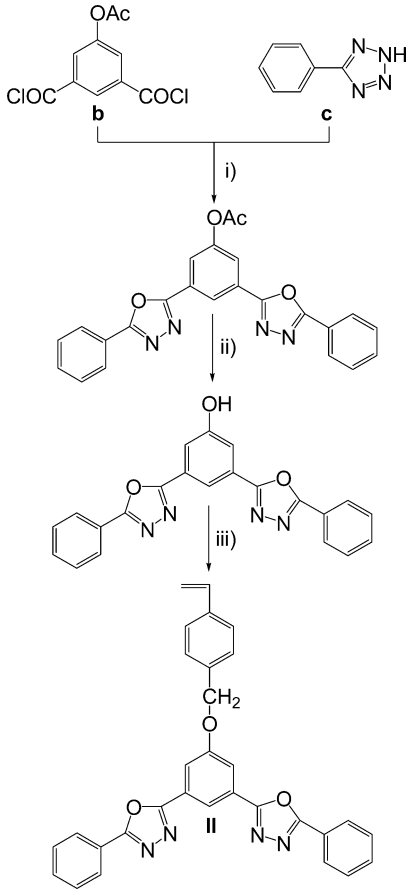

Scheme 3. (i) 2-Chloropropionyl Chloride (CPC), Et_3N, THF. (ii) Monomer I or II, CuBr, PMDETA or Bipy, Ph_2O, 110 °C.

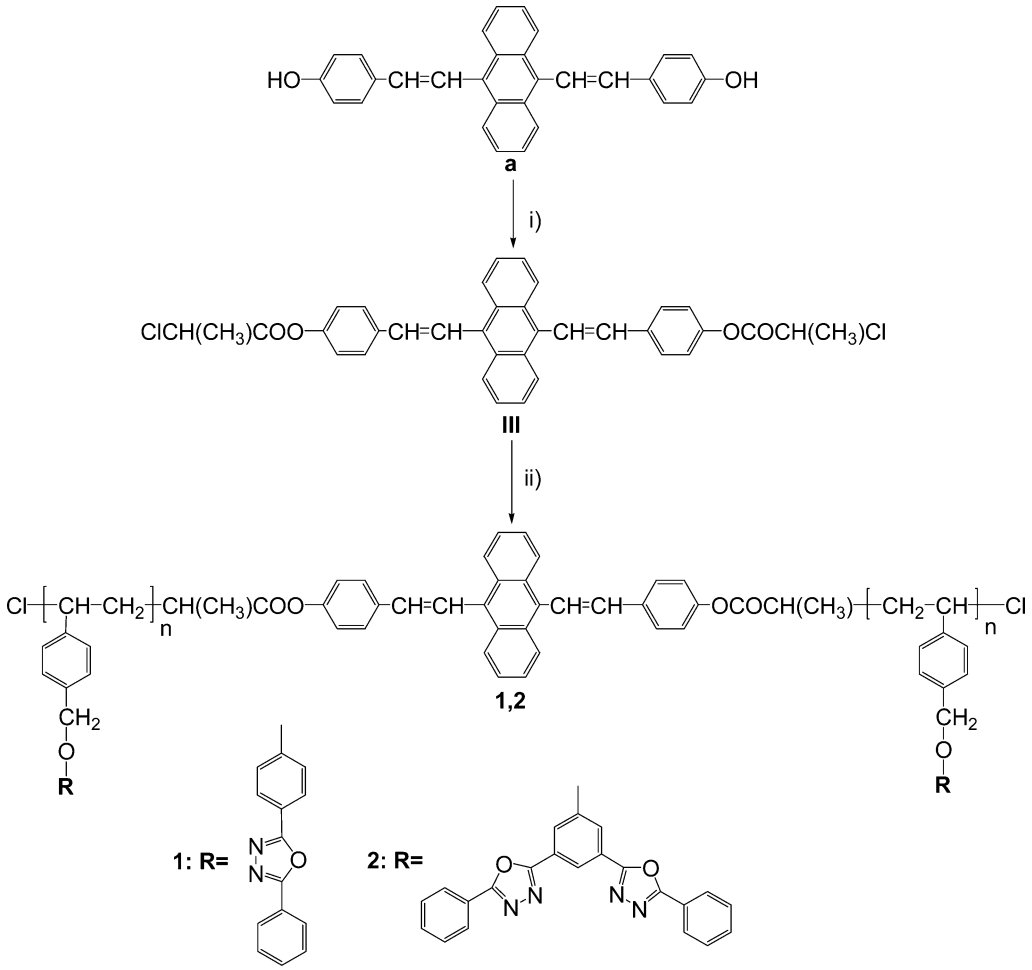

chromatography (GPC). In Figure 1 the ^1H NMR spectra of the initiator and of the copolymer **1ii** are presented. Most of the characteristic signals of the rigid block (Figure 1a) that are signals in the aromatic region in the range of $\delta = 6.9-7.4$ ppm can be clearly distinguished in the spectrum of the copolymer (Figure 1b). Moreover the signal at $\delta = 4.7$ ppm, which is assigned to the terminal protons next to the halogen atoms of the initiator, has totally disappeared after the polymerization. Additionally, the GPC chromatogram of **1ii** (Figure 2) using different wavelengths for detection, that is, 300 and 420 nm, supported this conclusion. While at 300 nm both blocks, di(styryl)-anthracene unit as the rod block and oxadiazole homopolymers as the flexible blocks, absorb light, at 420 nm only the di(styryl)-anthracene unit absorbs light. The GPC traces obtained show no significant difference, proving that the rigid initiator is incorporated into the polymers. Gel permeation chromatography was also used to make sure that no trace of unreacted initiator remained in the copolymers and to examine the effectiveness of the synthetic process in obtaining copolymers with narrow polydispersities. As shown in the inset in Figure 2, GPC does not reveal residual initiator. This indicates high initiation efficiency. The initial workup procedure (precipitation with methanol) is not expected to remove residual initiator because of the low solubility of the initiator in methanol. The homogeneity of the copolymers as stated previously was also assessed by gel permeation chromatography based on calibration with polystyrene standards. Chromatograms were recorded at the standard 254 nm. The copolymers were synthesized and their molecular characteristics are given in Table 1. The molecular weights of the rod−coil triblock copolymers **1** and **2** vary between 4300 and 22300 and 2300−6300 with 2.7−13.7 wt % and 9.4−26.1 wt % in styryl-anthracene units, respectively. The polydispersity indices (M_w/M_n) of the copolymers are in the range 1.17−1.66 and 1.47−1.65, respectively. A wide range of M_w was obtained, depending mainly on the catalytic system used, as shown in Table 1. Although bipyridine gave lower polydispersities, higher M_w copolymers were obtained with PMDETA (*N*,*N*,*N*′,*N*′,*N*″-pentamethyldiethylenetriamine) as the catalyst's ligand. In cases where PMDETA was used, broader molecular weight distributions were obtained.

Thermal Properties. The thermal properties of the initiator **III** and triblock coil−rod−coil copolymers **1v**, **1vi**, and **1vii** were examined using differential scanning calorimetry (DSC) and their thermograms are depicted in Figure 3. Glass transitions were detected between 103 and 122 °C for the copolymers **1** with a different percentage of di(styryl)-anthracene, and this was due to the different molecular weight of the flexible block. The copolymers **1v** and **1vi** also exhibit one endothermic peak at 231 and 218 °C, respectively, while the copolymer **1vii** does not show any endothermic transition. The decrease of the T_m of the rigid part as the percentage of

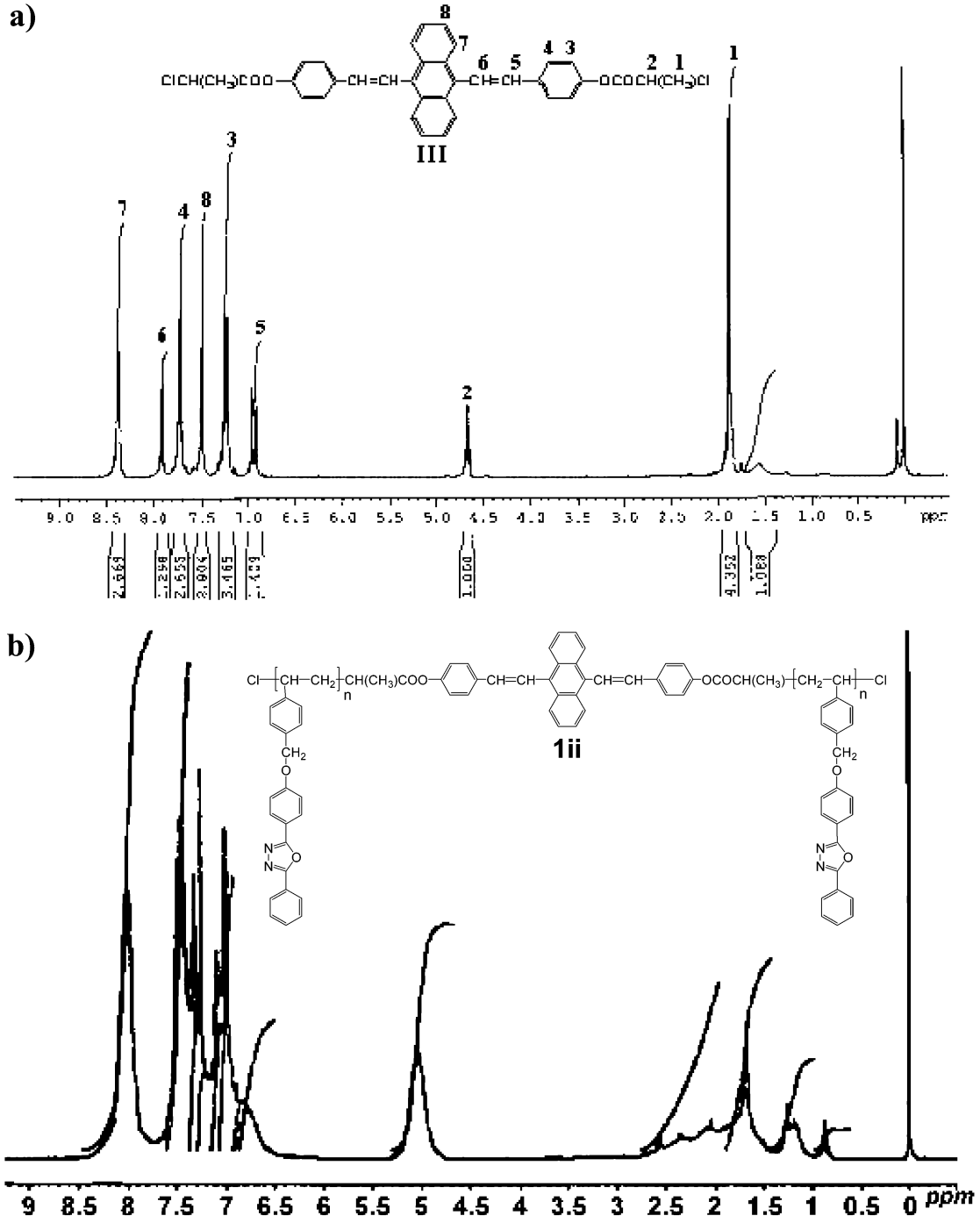

Figure 1. ^{1}H NMR spectra in $CDCl_3$ at room temperature of the initiator **III** and of the copolymer **1ii** with the assignment of the peaks of the initiator.

the flexible block is increased (copolymers **1v** and **1vi**) and the absence of crystallization in **1vii** shows that the crystallization ability of the rigid block is decreased as the flexible block is increased. The initiator shows two endothermic peaks at around 191 and 223 °C during the first heating scan.

Optical Properties. The optical properties of the coil−rod−coil copolymers in solution are a sum of the optical properties of the initiator and oxadiazole homopolymers. The inset in Figure 4 shows the UV−vis absorption spectra of the initiator **III**, of the side chain oxadiazole homopolymer, and of the triblock coil−rod−coil copolymers **1**, in $CHCl_3$ solutions. The absorption maxima of the oxadiazole-based part are at about 294−296 nm in both the homopolymer and triblock copolymers. The λ_{max} of the initiator part is at higher wavelengths (414 nm), corresponding to a more extensive conjugation. The homopolymer and triblock copolymers in the solid state show UV−vis absorption spectra similar to those observed for the respective polymer solutions (Figure 4). However, all the copolymers in the solid state show a 6−8 nm red shift in the absorption region of the oxadiazole-based part and a 4−14 nm red shift in the absorption region of the anthracene-based part, compared to those observed in solution. The red shift in the absorption is likely due to morphological reasons. The copolymers **2ii** and **2iii**, in $CHCl_3$ solutions, exhibit two absorption maxima at 266 and 280

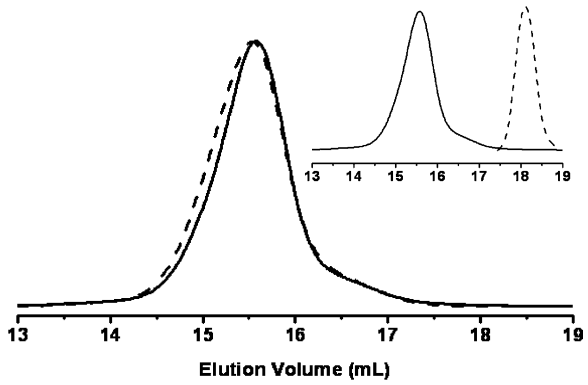

Figure 2. GPC chromatograms of the copolymer **1ii** in $CHCl_3$ recorded at 300 nm (solid curve) and 420 nm (dashed curve), respectively. The inset shows the GPC chromatograms of the copolymer **1ii** (solid curve) and of the initiator **III** (dashed curve) in $CHCl_3$ detected at 254 nm.

Table 1. Reaction Conditions and Molecular Weight Characteristics of the Synthesized Block Copolymers

		GPC results[d]			
polymer	amine	M_n	M_w	PDI	wt % in di(styryl)-anthracene unit
1i[a]	bipy	4330	5100	1.18	13.7
1ii[a]	bipy	5240	6140	1.17	11.3
1iii[a]	bipy	6260	8630	1.38	9.5
1iv[a]	PMDETA	8190	11620	1.42	7.3
1v[a]	PMDETA	8640	13840	1.60	6.9
1vi[b]	PMDETA	13700	22750	1.66	4.3
1vii[b]	PMDETA	22270	99490	4.47	2.7
2i[c]	PMDETA	2280	3620	1.59	26.1
2ii[a]	bipy	3880	6030	1.55	15.3
2iii[c]	PMDETA	5590	8240	1.47	10.6
2iv[c]	PMDETA	6300	10390	1.65	9.4

[a–d] Reaction conditions: [a]CuBr, diphenyl ether with 5% w/v ethylene carbonate (EC), 110 °C. [b]CuBr, diphenyl ether with 30% w/v ethylene carbonate (EC), 110 °C. [c]CuBr, diphenyl ether with 10% w/v ethylene carbonate (EC), 110 °C. [d]Molecular weights and polydispersity indices were determined with size exclusion chromatography ($CHCl_3$, room temperature) using polystyrene standards.

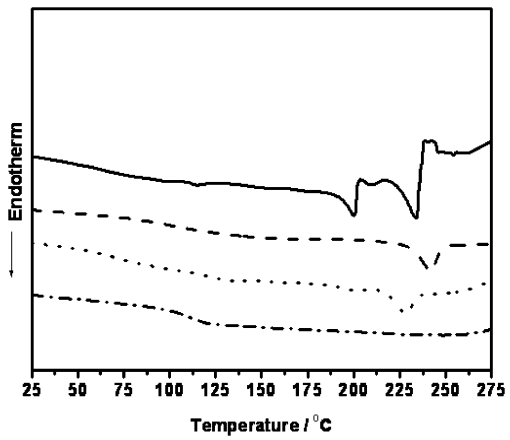

Figure 3. DSC thermograms of the initiator **III** (solid curve) (first run) and of the triblock copolymers **1v** (dashed curve), **1vi** (dotted curve), and **1vii** (dashed dot curve) (second run). The first and second heating rates were 20 °C min^{-1}.

nm, respectively, in the absorption region of the oxadiazole-based part (Table 2). Compared to the absorption data of the copolymers containing one oxadiazole ring per repeated unit, that is, **1ii**, the introduction of an additional oxadiazole ring in the copolymers **2ii** and **2iii** containing two oxadiazoles rings per repeated unit brings about a change to the absorption maxima of the

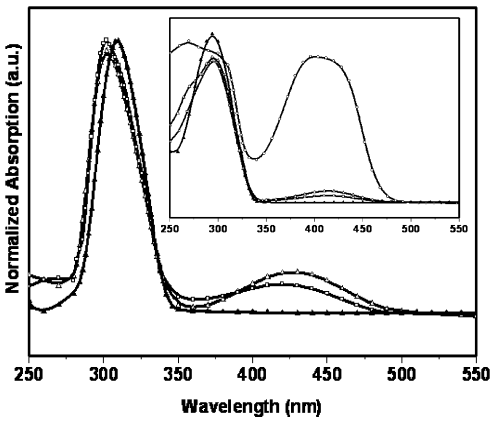

Figure 4. UV−vis absorption spectra of the side-chain oxadiazole homopolymer (solid triangles) and of the copolymers **1ii** (open triangles) and **1v** (open squares), in solid state. The inset shows the UV−vis absorption spectra of the initiator **III** (open circles), of the side-chain oxadiazole homopolymer, and of the copolymers **1ii** and **1v**, in $CHCl_3$ solutions.

Table 2. Absorption and Emission Spectral Data of the Copolymers in Chloroform Solutions and in Solid State

polymer	λ_{abs}[a] (nm) solution	λ_{abs}[a] (nm) film	λ_{PL}[a,b] (nm) solution	λ_{PL}[a,b] (nm) film	λ_{PL}[a,c] (nm) solution	λ_{PL}[a,c] (nm) film
1ii	296, 414	302, 428	354, 535	512	537	512
1iii	296, 414	302, 420				
1v	296, 414	302, 418	354, 535	512	537	512
1vi	294	302, 438				
1vii	294	302, 448				
2ii	266, 416	300, 426				
2iii	280, 416	302, 430	358, 522		524	

[a] Wavelength of maximum absorbance or emission, wavelength of the shoulder peak is in brackets. After excitation at the maxima of the absorption bands [b]of the oxadiazole moiety and [c]the conjugated rigid block.

oxadiazole-based part in the short wavelength region. Both the copolymers in the solid state show red-shifted absorption maxima compared to those observed in solution (Table 2). More specifically, the copolymers **2ii** and **2iii** show a 22−34 nm red shift in the absorption region of the oxadiazole-based part and a 10−16 nm red shift in the absorption region of the anthracene part, respectively. The higher red shift of the oxadiazole peak maxima in these copolymers compared to the mono-oxadiazole copolymers is probably due to the higher tendency of this structure to interact, resulting in more efficient aggregate formation.

Figure 5 gives the photoluminescence spectra of the initiator **III** and of the copolymers **1ii** and **2iii**, in $CHCl_3$ solutions of 1×10^{-4} M. The photoluminescence spectra were obtained after excitation at the absorption maxima of the oxadiazole moiety (300 nm) (Figure 5a**)** and of the conjugated rigid block (420 nm) (Figure 5b**)**. The two different oxadiazole-containing copolymers exhibit the same behavior, after excitation at the absorption maximum of the oxadiazole moiety, since the molecular weights of the flexible blocks are comparable. Comparing the emission peak maxima at about 520 nm, it is obvious that copolymer **1ii** is red-shifted (535 nm) compared to copolymer **2iii** which show emission at 522 nm. Since the molecular structure of this copolymer does not contain any additional conjugated segment that could be responsible for the observed red shift, we conclude that this behavior must be due to aggregate

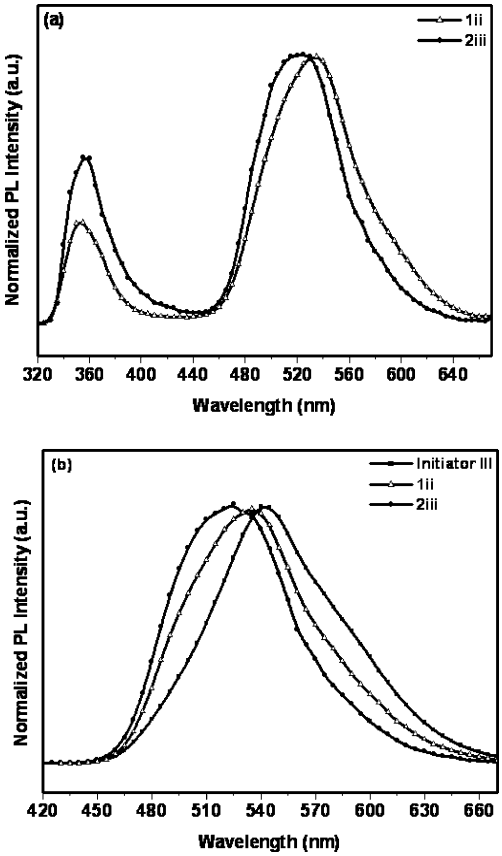

Figure 5. Photoluminescence spectra of the initiator **III** (solid squares) after excitation at 420 nm and of the prepared copolymers **1ii** (open triangles) and **2iii** (solid circles) after excitation (a) at 300 nm (b) and at 420 nm in $CHCl_3$ solutions of 1×10^{-4} M.

formation being more predominant in this copolymer. Excitation at 420 nm in solution resulted in an emission at about 520 nm obtained from the two copolymers studied (Figure 5b). The emission maxima of the copolymers **1ii** and **2iii** are located at 537 and 524 nm, respectively, as shown in Table 2. The energy transfer initially observed in solution for the copolymers studied becomes much more efficient in the solid state where the copolymers emit in the green spectral region (at about 520 nm) regardless of the excitation wavelength, as shown for example in Figure 6 for the copolymer **1ii**. The origin of this energy transfer can be attributed to the fact that the emission maxima of the blue-emitting segment (homopolymer) at about 360 nm overlaps with the absorption maximum of the initiator resulting in emission only from the latter unit. The absorption and emission spectral data of the copolymers in solution and of films cast from solution in $CHCl_3$ are summarized in Table 2. The optical properties of nitrogen heterocycles are known to be influenced by protonation. The influence of an acid upon the optical properties of the oxadiazole-containing polymers has been recently studied[27] and a significant quenching of the emission was observed by the addition of an organic acid into a polymeric solution. Addition of an acid into a chloroform solution with different copolymer concentrations, namely, 10^{-6} and 10^{-4} M, was studied for the copolymer **1ii** and the results are shown in parts (a) and (b), respecively,

(27) Wu, T.-Y.; Sheu, R.-B.; Chen, Y. *Macromolecules* **2004**, *37*, 725.

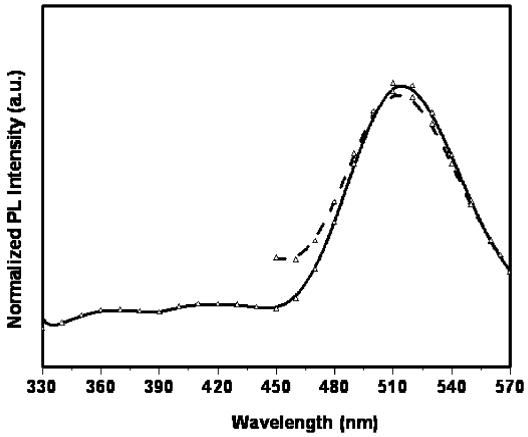

Figure 6. Photoluminescence spectra of the copolymer **1ii** in solid state. Excitation wavelengths were 300 nm (solid curve) and 420 nm (dashed curve).

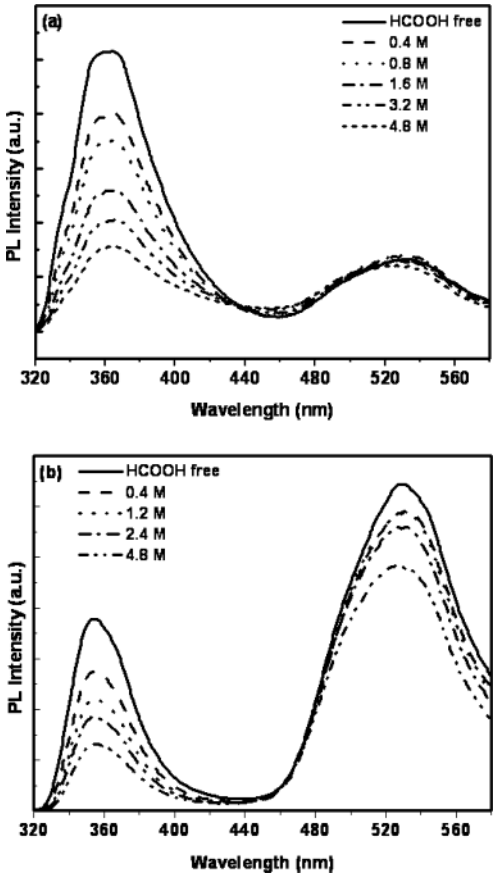

Figure 7. Photoluminescence spectra of the copolymer **1ii** in chloroform solution of (a) 1×10^{-6} and (b) 1×10^{-4} containing different concentrations of formic acid. Excitation wavelength was 300 nm.

of Figure 7. As the solution concentration was increased, the relative ratio of the two peaks at about 360 and 520 nm was changed, giving indication that energy transfer occurred in the concentrate solution, resulting in a more intensive peak at 520 nm. Moreover, in both cases, addition of formic acid gives rise to significant quenching of the emission peak at 354 nm, while in the case of 10^{-6} M polymer solution there is no significant effect on the emission peak at 535 nm (Figure 7a).For the concentrated solution (10^{-4} M) there is a small decrease of the emission peak at 535 nm, as shown in Figure 7b. Since the peak at 535 nm cannot be influenced from the

acid addition, the small decrease observed in its intensity (Figure 7b) further supports the idea of energy transfer in these systems even in solution.

Conclusions

Coil−rod−coil copolymers having different combinations of oxadiazole-based monomers have been synthesized using atom transfer radical polymerization. In most cases copolymers with low polydispersities were obtained. The study of the optical properties in solution and in solid state revealed an efficient energy transfer from the UV-emitting moieties to the green-light-emitting units. This energy transfer was also shown to exist in solution but it was more efficient in the solid state, resulting thus in green light emission from all the copolymers studied. This method enabled us to combine the electron-transporting properties of the oxadiazole blocks with the optical properties of the conjugated part, which can also be fine-tuned by proper selection of the structure of the rigid part of the copolymers.

Acknowledgment. This work was partially supported by the Operational Programme for Education and Initial Vocational Training on “Polymer Science and Technology” 3.2a, 33H6, administered through the Ministry of Education in Greece.

CM049670K